Structural Plasticity and Rapid Evolution in a Viral RNA Revealed by In Vivo Genetic Selection[∇][†]

Rong Guo,[1] Wai Lin,[2] Jiuchun Zhang,[1] Anne E. Simon,[1] and David B. Kushner[2]*

Department of Cell Biology and Molecular Genetics, University of Maryland—College Park, College Park, Maryland 20742,[1] and Department of Biology, Dickinson College, Carlisle, Pennsylvania 17013[2]

Satellite RNAs usually lack substantial homology with their helper viruses. The 356-nucleotide satC of Turnip crinkle virus (TCV) is unusual in that its 3′-half shares high sequence similarity with the TCV 3′ end. Computer modeling, structure probing, and/or compensatory mutagenesis identified four hairpins and three pseudoknots in this TCV region that participate in replication and/or translation. Two hairpins and two pseudoknots have been confirmed as important for satC replication. One portion of the related 3′ end of satC that remains poorly characterized corresponds to juxtaposed TCV hairpins H4a and H4b and pseudoknot ψ_3, which are required for the TCV-specific requirement of translation (V. A. Stupina et al., RNA 14:2379–2393, 2008). Replacement of satC H4a with randomized sequence and scoring for fitness in plants by in vivo genetic selection (SELEX) resulted in winning sequences that contain an H4a-like stem-loop, which can have additional upstream sequence composing a portion of the stem. SELEX of the combined H4a and H4b region in satC generated three distinct groups of winning sequences. One group models into two stem-loops similar to H4a and H4b of TCV. However, the selected sequences in the other two groups model into single hairpins. Evolution of these single-hairpin SELEX winners in plants resulted in satC that can accumulate to wild-type (wt) levels in protoplasts but remain less fit in planta when competed against wt satC. These data indicate that two highly distinct RNA conformations in the H4a and H4b region can mediate satC fitness in protoplasts.

Defective interfering (DI) and satellite (sat) RNAs are subviral RNAs that associate with viruses, require virus-encoded proteins for replication and other activities, and are capable of modifying viral infections. DI RNAs, found primarily in infections of animal hosts, are generated from viral genomic sequence, while satRNAs, more common to plant viruses, feature sequence that usually is unrelated to the helper virus. Most of the subviral RNAs with limited genome sizes are not translated, and thus their effect on virus infection must be mediated by the RNA primary or higher-ordered structure. DI and satRNAs that associate with different positive-strand RNA viruses can either intensify or attenuate viral symptoms (3, 10), which can involve inhibition of virus-encoded posttranscriptional gene silencing suppressors (9) or activation of posttranscriptional gene silencing (23).

satRNAs and DI RNAs that share partial or near-complete sequence similarity with their helper virus contain related regions that allow for recognition by the helper virus RNA-dependent RNA polymerase (RdRp). While this had led to the supposition that subviral RNAs would be useful models for examining replication elements that also exist in the much larger helper virus genome, more recent findings that RNA viruses contain elements in both their 5′ and 3′ untranslated regions that participate in translation (11, 15, 16), a function not required by small subviral RNAs, suggest that subviral

RNAs might evolve to differentially use genomic-derived sequences that are no longer required for helper virus-related functions. Elucidation of such functional differences in the utilization of shared sequences could therefore lead to important insights into the relationship between viral and associated subviral RNAs.

Turnip crinkle virus (TCV) is a member of the genus *Carmovirus* within the family *Tombusviridae*. TCV contains a single 4,054-nucleotide (nt) genomic RNA that encodes proteins important for RNA-dependent RNA replication (p28 and p88), movement (p8 and p9), and encapsidation/RNA silencing suppression (CP) (8, 18, 30) (Fig. 1A). TCV is also associated with two satRNAs, satD and satC (22) (Fig. 1A), one of which (satC) modifies TCV infection by reducing viral RNA accumulation while enhancing TCV-induced symptoms (23). With the exception of its extreme 3′ end, the 194-nt satD lacks consecutive sequence homology with TCV. satC (356 nt) is a unique satellite in that it is a chimera related to nearly full-length satD at its 5′ end and two regions from TCV including 150 3′ coterminal bases at its 3′ end (Fig. 1A). Because of the high degree of sequence similarity and MPGAfold-based prediction of structural similarity between the 3′ ends of satC and TCV (13, 37) (Fig. 1B), satC was considered a good model for understanding *cis*-acting sequences that participate in the replication of TCV. However, recent identification of a 3′-proximal translational enhancer (26) partially contained within the shared region that is necessary for gene expression of TCV, but not satC, has complicated assignment of element function and/or importance based on sequence and structural conservation. In addition, recent findings that the satC 3′ end adopts several different conformations (preactive and active structures that control initiation of minus-strand synthesis [35, 39]) fur-

* Corresponding author. Mailing address: Department of Biology, Dickinson College, P.O. Box 1773, Carlisle, PA 17013. Phone: (717) 245-1328. Fax: (717) 245-1130. E-mail: kushnerd@dickinson.edu.
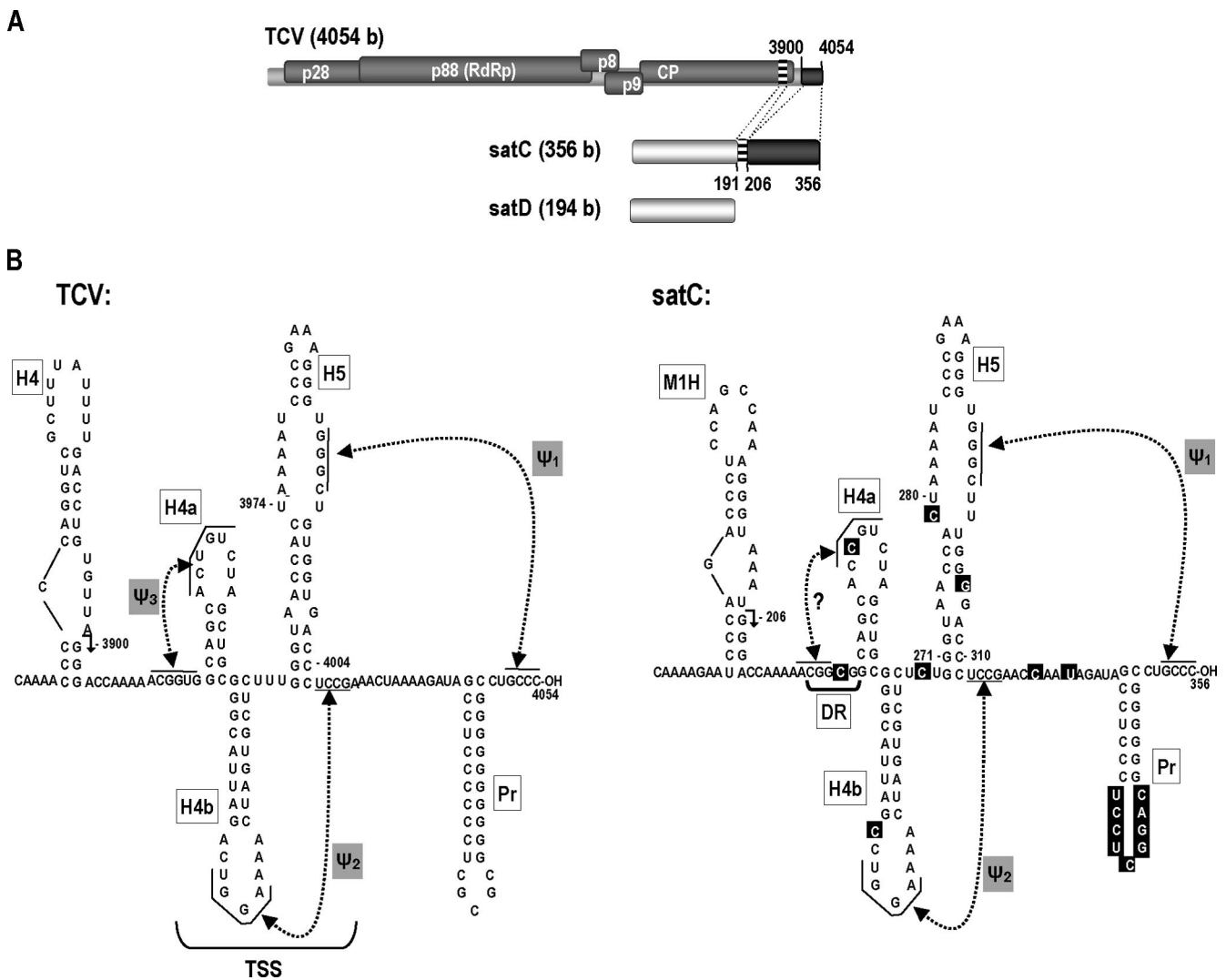
FIG. 1. Relationship between TCV and satC. (A) Schematic representation of TCV-associated RNAs. The single plus-strand genome of TCV and five open reading frames are shown. p28 and the readthrough protein p88 (the RdRp) are required for replication. p8 and p9 are required for cell-to-cell virus movement. CP is the coat protein open reading frame. satC is a chimeric RNA composed of a second satRNA (satD) and two regions from the 3′ end of TCV. Numbers and dotted lines indicate which satC sequences are shared with TCV. Similar regions are shaded similarly. (B) MPGAfold-predicted TCV and satC 3′ structures. MPGAfold predicts a slightly different H4a and associated pseudoknot for satC than the one depicted (see Fig. 3A, right). Hairpins and pseudoknots are described in the text. The DR is an important element required for a conformational switch that activates the template. The region that folds into a TSS in TCV is indicated. Arrowheads in H4 and M1H denote the 5′ ends of shared 3′-terminal sequences. The ? denotes that formation of ψ₃ in satC has not been established. Sequence differences between satC and TCV are boxed in the satC sequence. Although the satC structure is shown in a similar configuration as TCV for ease of comparison, none of the hairpins or ψ₁ is present in the satC structure assumed by transcripts synthesized in vitro, while at least H5 and ψ₁ are present in the satC replication-active structure (35, 38).

ther complicate determining the existence and importance of satC structures.

As shown in Fig. 1B, satC and TCV are capable of forming a similar set of hairpins and pseudoknots (13). From 3′ to 5′ these hairpins are Pr, H5, H4b, and H4a. Pr, found in 10 of 11 carmoviruses, is the core promoter for minus-strand synthesis for satC (25) and TCV (28). H5, found in 10 of 11 carmoviruses, is thought to be a chaperone for the viral RdRp (12) and forms a pseudoknot (ψ_1) with 3′-terminal residues (36, 37, 40). Pr, H5, and ψ_1 have been confirmed as important for accumulation of both TCV and satC (12, 13, 25, 37, 38, 40). H4b, predicted to be present in some carmoviruses, is important for

robust accumulation of TCV and participates in an important pseudoknot (ψ_2) between its terminal loop and sequence flanking the 3′ side of hairpin H5 in TCV (13). While H4b has not been confirmed for satC, ψ_2 is important for robust satC accumulation (39). In TCV, H4a and the H-type pseudoknot ψ_3, which forms between the H4a loop and upstream flanking sequences, are important for translation (26) and also RdRp binding to the region (M. Young and A. E. Simon, unpublished data). The fragment encompassed by ψ_3 and ψ_2 in TCV was recently shown to comprise a functional unit that is predicted to fold into a T-shaped structure (TSS) and binds to 80S ribosomes and 60S ribosomal subunits (13, 26). The analogous

region in satC, however, was predicted to be incapable of assuming the TSS and also was not a template for ribosome binding (26).

Based on biochemical structure mapping, the preactive structure of satC does not contain hairpins H4a, H4b, H5, or Pr or pseudoknot ψ_1, but does contain ψ_2 (35). However, in vivo genetic selection (SELEX) revealed that the structures and some sequences within Pr and H5 are critical for satC accumulation in plants and protoplasts (1, 39, 40). In addition, fragment exchanges with the related carmovirus *Cardamine chlorotic fleck virus* (CCFV) suggested that H4a and H4b form a functional unit in satC (39). The sequence just upstream of H4a, known as the derepressor (DR), appears to be important for the conformational switch between preactive and active structures (35, 37). However, whether the DR participates in a ψ_3-type interaction as it does in TCV is not known.

Using mutagenesis and SELEX, we now report that formation of ψ_3 is not important for satC replication but cannot be excluded from having a role in satC-helper virus interactions. In addition, we have determined (i) in the presence of wild-type (wt) H4b, sequence in the H4a region is selected to form an H4a-like stem-loop, (ii) the DR can function in an alternative location and can exist as part of the stem of H4a, and (iii) satC H4a and H4b are functional either as two adjacent stem-loops (as is the case in wt satC) or as a single hairpin, with little sequence similarity to wt satC required. This suggests that given the opportunity, viral RNAs can rapidly evolve topologically distinct elements to perform similar functions.

MATERIALS AND METHODS

In vivo SELEX. In vivo genetic selection was performed as previously described (1). To generate the template for in vitro transcription of satC with random sequence in place of the 18-nt H4a region (positions 222 to 239), two fragments were generated by separate PCRs with pC(+) (pUC19 containing full-length satC cDNA) as a template. The 5' fragment was produced by using primers T7C5', which contains a T7 polymerase promoter at its 5' end, and H4aL3' (for all oligonucleotides used in this study, see Table S1 in the supplemental material). The 3' fragment was generated by using primers BstE25' and oligo 7, which is complementary to the 19 nt at the 3' end of satC. To generate satC with a randomized H4a+H4b region (positions 222 to 266), separate PCRs using pC(+) and either oligos T7C5' and H4aH4bL3' or oligos BstE25' and oligo 7 were performed. PCR products were subjected to electrophoresis, purified using QIAQuick MinElute columns (Qiagen, Valencia, CA), digested with BstEII (all enzymes from New England Biolabs, Ipswich, MA, except where noted), phenol-chloroform extracted, and ligated together to produce full-length satC cDNA. These satC cDNAs with randomized H4a or H4a+H4b were in vitro transcribed using T7 RNA polymerase; TCV genomic RNA was in vitro transcribed from SmaI-linearized pT7TCVms (17). Both satC and TCV genomic RNA transcripts contain precise 3' and 5' ends. For the first round of selection, 2 µg of wt TCV transcripts and 5 µg of satC transcript with specific randomized sequences were inoculated onto each of 30 turnip seedlings (Turnip Hybrid Just Right; Gurney's, Greendale, IN). Total RNA was isolated from uninoculated leaves after 21 days and added to six new turnip seedlings for an additional 21-day infection; this was repeated for a total of five rounds. For rounds 1, 2, 3, and 5, satC RNA was reverse transcribed, amplified by PCR in the presence of Pyrostase polymerase (Molecular Genetic Resources, Tampa, FL) using primers T7C5' and oligo 7, cloned into SmaI-linearized pUC19, and subjected to sequencing (Penn State College of Medicine Molecular Genetics Core Facility, Hershey, PA, or Clemson University Genomics Institute, Clemson, SC). Selected round 3 H4a+H4b "winner" sequences were transcribed from their pUC19-based plasmids and self-evolved in plants (in the presence of TCV genomic RNA) for six rounds; RNA was reverse transcribed, cloned, and sequenced after rounds 1 and 6. Selected round 3 H4a+H4b "winner" sequences and selected "winners" from the sixth round of self-evolution also were subjected to direct competition in six turnip seedlings with RNA reverse transcribed, cloned, and sequenced 21 days later. Competition experiments between wt satC and SELEX

winners were as described previously (37). For competitions involving wt satC, control experiments were simultaneously performed in which individual plants were coinfected with TCV RNA and RNA of each satC SELEX winner, to verify that the satC transcripts were functional and able to be cloned in the absence of competition with wt satC. To obtain clones of satC with randomized H4a or H4a+H4b for use as controls in protoplast experiments, ligated satC cDNAs (described above) were directly cloned into the SmaI site of pUC19.

Accumulation of viral RNAs in protoplasts. TCV genomic RNA and satC transcripts were in vitro transcribed with T7 RNA polymerase using either plasmids pT7TCVms and pT7C(+) that were linearized with SmaI (24) or directly from PCR products. Protoplasts (5×10^6) prepared from callus cultures of *Arabidopsis thaliana* ecotype Col-0 were inoculated with 20 µg of TCV genomic RNA transcripts with or without 2 µg of satC RNA transcripts using polyethylene glycol-CaCl$_2$, as described previously (39). Total RNA isolated from protoplasts at 40 h postinoculation (hpi) was subjected to RNA gel blot analysis. This 40-h time point was used since accumulation of RNA is not saturating (32). The RNA was probed with [γ-^{32}P]ATP-labeled oligonucleotide oligo 13, which is complementary to positions 3950 to 3970 of TCV genomic RNA and positions 250 to 269 of satC, or [γ-^{32}P]ATP-labeled oligo 7, which is complementary to positions 338 to 356 of satC.

Site-directed mutagenesis of satC. After three rounds of evolution of satCs containing randomized H4a+H4b, two sequences (termed K$_{ab}$ and Q$_{ab}$) (see Fig. 5, below) were similar yet accumulated to different levels in protoplasts. Using the plasmid containing cloned satC sequence Q$_{ab}$ as template, four site-directed mutagenesis reactions (QuikChange Lightning kit; Stratagene, La Jolla, CA) using eight oligonucleotides (see Table S1 in the supplemental material) were performed; candidate plasmids were sequenced (Clemson University Genomics Institute, Clemson, SC) to verify that the desired changes, and no second-site mutations, were present. For the generation of plasmids m228-231, m219-222, m219-222/m228-231, C220G, G230C, C220G/G230C, m216-219, m216-219/m228-231, G219C, C228G, G219C/C228G, G218C, C229G, G218C/C229G, Δ216-220, m216-219/C229G, C229G/Δ216-220, C226U, C243U, and C243U/G263A, PCRs were performed with a common 5' primer (T7C5') homologous to the 5' end of template pT7C(+). The specific 3' primers are listed in Table S1 of the supplemental material. SpeI- (or BstEII for C243U/G263A) and NcoI-digested PCR products were ligated into similarly digested pT7C(+), replacing the endogenous fragment. For construction of plasmid G230C, PCR products were treated with SpeI and SnaBI, and fragments were inserted into the analogous location in SpeI and SnaBI digested pT7C(+). To obtain pG263A and pC226U/G263A, pT7C(+) and pC226U were treated with NcoI and SpeI, and the small fragments were purified and then ligated into NcoI/SpeI-digested pC243U/G263A vector backbone. To construct pC226U/C243U/G263A, PCR was performed using template pC226U and primers T7C5' and C243U/G263A. The PCR product was digested with NcoI and BstEII and ligated into similarly digested pT7C(+) vector backbone. All constructs were confirmed by DNA sequencing.

RESULTS

In vivo evolution of the satC H4a region results in retention of a stem-loop. Deletion of H4a from satC markedly impairs satC accumulation in protoplasts (39). In addition, fragment exchanges with the related CCFV revealed that H4a and H4b behave as a functional unit in satC (39). To further explore the sequence/structural requirements of satC H4a and H4b and their interrelationship, H4a was subjected to in vivo genetic selection (SELEX). satC with 18 randomized bases (positions 222 to 239) replacing H4a was transcribed and RNA was inoculated onto 30 turnip seedlings along with TCV genomic RNA. Since satC increases the rate of helper virus movement (33; F. Zhang and A. E. Simon, unpublished data), satCs possessing sequence in the H4a region that allow for its amplification are at a selectable advantage for accumulation with the helper virus in systemically infected leaves. After 3 weeks, RNA was extracted from new leaves excised from each of the 30 plants. Five distinct sequences (A, C and B, K, L, and N) were recovered from five different plants (Fig. 2A). With the exception of sequence A, each round 1 sequence could be
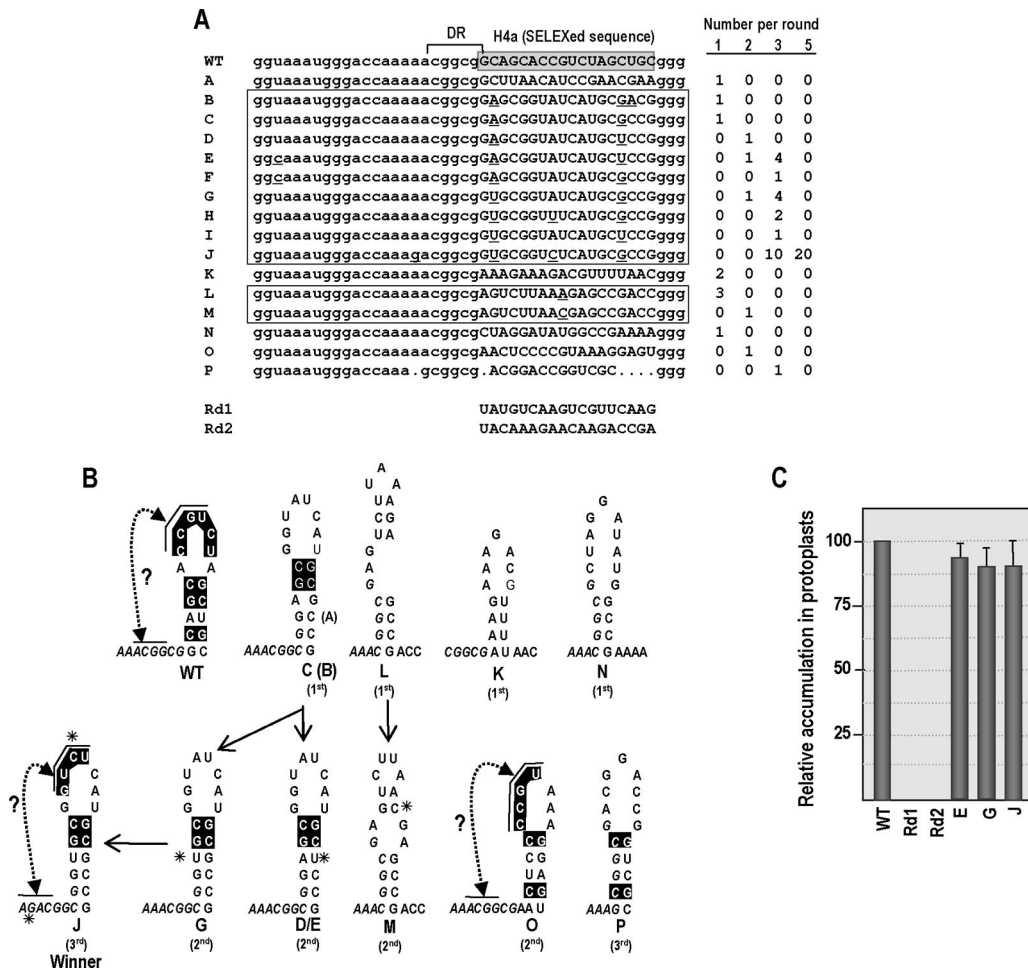
FIG. 2. In vivo genetic selection with randomized 18 nt of satC H4a results in retention of a stem-loop. (A) satC sequences obtained after SELEX rounds 1, 2, 3, and 5. Lowercase letters indicate nucleotides upstream and downstream of SELEXed H4a. A through P represent 16 distinct cloned sequences, with related sequences boxed; underlined nucleotides in the H4a region of these boxed sequences denote differences between the related clones. Underlined nucleotides in the region 5′ of H4a indicate changes from wt. Two random (nonselected) H4a sequences (Rd) are shown. (B) Modeled stem-loops of various cloned sequences. Potential pseudoknots in wt, O, and J are noted by arrows pointing to complementary sequence. Italicized nucleotides at the 5′ ends of the sequences denote non-H4a sequence. Asterisks in E, G, J, and M denote base changes from the progenitor sequence. Black boxes (wt, C, E, G, J, O, and P) indicate identical nucleotides between wt and respective SELEX sequences. The single nucleotide difference between sequence B and C is enclosed by parentheses. The round in which the SELEXed sequence was first cloned is noted below each modeled structure. (C) Accumulation in protoplasts 40 h postinfection of wt satC, H4a SELEX sequences E, G, and J, and satC with random (Rd1 or Rd2) H4a sequences. Results from three independent experiments were normalized to wt satC levels. Standard deviations are indicated.

modeled to form a single stem-loop with stems of 4 to 5 bp, with some hairpins requiring incorporation of a portion of the upstream DR sequence (Fig. 2B). None of the selected sequences exhibited extensive sequence similarity with wt H4a, with only related sequences C and B having two consecutive base pairs closing the terminal loop that were identical to satC.

To ascertain which round 1 satC was more fit and to allow for further evolution, total RNA preparations from all 30 round 1 plants were combined and the pooled mixture of satRNAs and TCV genomic RNA was inoculated onto six new turnip seedlings. At 21 days postinoculation, total RNA was extracted, combined, and reinoculated onto six additional seedlings. These steps were repeated for a total of five rounds, with satC cloning and sequencing performed for rounds 2, 3, and 5. As shown in Fig. 2A, none of the round 1 sequences

were precisely maintained in round 2. Round 2 sequences D, E, and G were derived from first-round sequence C, with E differing from D by a U-to-C second-site alteration at position 201 in the upstream hairpin M1H (Fig. 1B). Sequence M differed from first-round progenitor sequence L by a single nucleotide. Sequence O was newly identified in round 2 but was not isolated in further rounds. All five round 2 sequences could form more stable wt H4a-like stem-loops than the first-round sequences (Fig. 2B).

In round 3, sequences E and G were again isolated, along with similar sequences F, H, I, and J, indicative of continued evolution of this group. Sequence J contained 4 nt in the H4a loop that were identical to the similarly placed sequence in wt H4a. Sequence P, featuring a shortened, 13-nt-long H4a, was isolated once (Fig. 2B). Sequence J emerged as a SELEX

winner, as it comprised nearly one-half of the sequenced clones for round 3. By round 5, only sequence J was isolated, making it the functional winning sequence in this experiment. Mfold (41) prediction of full-length satC with sequence J in place of H4a suggests that sequence J can fold into a stem-loop, as modeled in Fig. 2B (data not shown).

The emergence and evolution of sequence J in plant infection could reflect more robust replication or an enhanced ability to support rapid TCV movement (33). To determine if sequence J was capable of enhanced replication in protoplasts compared with related sequences not found in later rounds, wt satC, sequences E, G, and J, and two satCs with random H4a sequences (Rd1 and Rd2) (Fig. 2A) cloned from the initial population of randomized H4a sequences prior to SELEX in plants were individually inoculated into protoplasts along with TCV genomic RNA and assessed 40 h later for plus-strand accumulation. Rd1 and Rd2 did not accumulate to detectable levels, indicating the importance of specific sequences/structures in this region for satC amplification. In contrast, satC with H4a sequences E, G, and J accumulated to nearly wt levels (Fig. 2C). Altogether, these results strongly suggest that a hairpin in this region contributes to replication of satC. However, lack of detectably enhanced accumulation by winning sequence J compared to related sequences E and G suggests that the two unique alterations in sequence J in the H4a loop (position 229) and upstream H4a-flanking (not SELEXed) sequence (position 215) contribute to a different satC attribute that allows for its strong selection by the helper virus in infected plants.

ψ₃ is not required for satC accumulation in protoplasts. The two new alterations in sequence J that enhance fitness in planta compared with progenitor sequence G would allow for a pseudoknot to form (Fig. 2B) that is similar to TCV ψ₃ (Fig. 1B). ψ₃ is critical for TCV translation (26) and is also involved in RdRp binding to the TCV 3′ end in vitro (Young and Simon, unpublished). Sequence O, which was present in the second-round SELEX, also has the potential of forming a similar TCV-like pseudoknot. When wt satC was subjected to structural computational analysis with MPGAfold (20, 21), an H-type pseudoknot was predicted to occur in the DR/H4a region that differs slightly from TCV ψ₃ (Fig. 3A, left and right, respectively). The H4a-like hairpin was predicted to contain a 3-bp stem capped by a 9-nt loop, with four residues from the loop predicted to pair with upstream DR sequences. RNA biochemical mapping of the DR region in full-length satC transcripts revealed only faint susceptibility to single-stranded specific enzymes, suggesting that the DR is located in a paired or stacked configuration (35), which is consistent with both structures.

To examine whether either pseudoknot is important for amplification of wt satC in protoplasts, single and potentially compensatory exchanges were introduced into H4a and the upstream DR sequence. Converting positions 228 to 231 from CCGU to GGCA in the loop of the MPGAfold-predicted hairpin (m228-231) (Fig. 3A, left) reduced satC accumulation to 46% of wt levels (Fig. 3B). Altering upstream DR residues 219 to 222 from GCGG to UGCC (m219-222) (Fig. 3A, left) reduced satC accumulation to 4% of wt (Fig. 3B), supporting previous results that alterations in the DR can be highly deleterious (39). Combining both 4-nt alterations, which is pre-
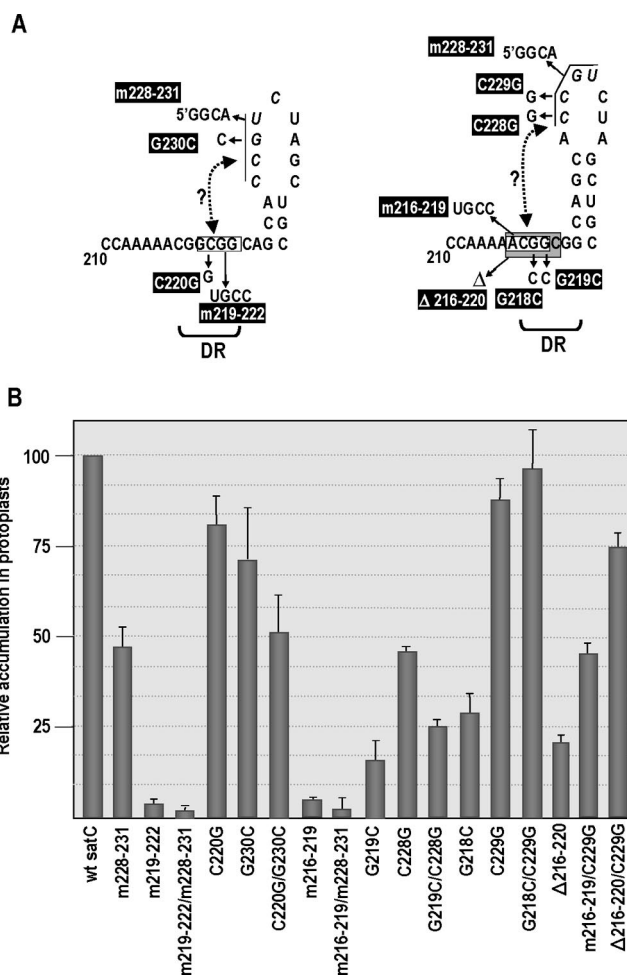

FIG. 3. ψ₃ is not required for satC replication in protoplasts. (A) satC pseudoknot predicted by MPGAfold (left) or similar to TCV ψ₃ (right). Nucleotides involved in a putative pseudoknot are italicized in the loop and connected to their putative interacting sequences by a hatched line with a double arrowhead. Mutant designations are boxed in black; altered bases in mutagenesis experiments are indicated. (B) Accumulation of satRNA (with various mutations) in protoplasts at 40 h postinfection. Mutations are shown in panel A. Data from at least three independent experiments were normalized to wt satC levels. Standard deviations are indicated.

dicted to reform the putative pseudoknot in the MPGA-predicted structure, reduced accumulation of the mutant satC to 2% of wt, and thus did not support this pseudoknot. Converting only the cytidylate at position 220 to a guanylate (C220G) and the putative MPGAfold-predicted partner guanylate at position 230 to a cytidylate (G230C) resulted in more limited negative effects on accumulation (80% and 67% of wt, respectively) (Fig. 3B). satC containing both C220G and G230C accumulated to 51% of wt, again indicating that the combined alterations were not compensatory. Therefore, these exchanges do not support the MPGAfold-predicted pseudoknot.

To examine if a TCV-like ψ₃ interaction is important for amplification of wt satC in protoplasts, positions 216 to 219 were converted from ACGG to UGCC (m216-219), which would be putatively compensatory with m228-231 (Fig. 3A, right). m216-219 alone or combined with m228-231 accumu-

lated to 5% and 2% of wt, respectively (Fig. 3B). Two sets of single and dual exchanges were also introduced into the region to test for the presence of a TCV-like ψ_3. G219C reduced satC accumulation to 15% of wt, while putative partner C228G reduced satC accumulation to 45% of wt. satC containing the combined alterations accumulated to 25% of wt. Alteration of position 218 (G218C) reduced satC accumulation to 28% of wt, as previously reported (35). Putative partner mutation C229G did not substantially affect satC levels (87% of wt). Interestingly, combining the two alterations (G218C/C229G) (Fig. 3A, right) restored satC accumulation to 96% of wt (Fig. 3B), suggesting that C229G was able to compensate for the low accumulation due to G218C.

One possible interpretation of this latter result is if the negative effect of the G218C alteration in the DR region (G CCGCC) was compensated by a fortuitous generation of a sequence with properties of the DR sequence (i.e., GCC) in the loop of H4a when C229 was converted to a guanylate. The validity of this interpretation was tested by addressing if the C229G alteration could compensate for other modifications in the DR that together would not be compensatory for reestablishment of a pseudoknot. The DR modifications tested were m216-219 and a new construct with a deletion of 5 nt (ACGGC; Δ216-220) (Fig. 3A, right). Δ216-220 reduced satC accumulation to 22% of wt (Fig. 3B). When combined with m216-219 or Δ216-220, C229G restored accumulation to 45% or 75% of wt, respectively (Fig. 3B). These results strongly suggest that generation of a new, partially functional DR element downstream from the original element can compensate in part for DR alterations, indicating that the DR has some flexibility in its location. Altogether, these data do not support either pseudoknot as important for replication of satC. However, based on the fitness of sequence J in plants, a nonreplication effect of a pseudoknot in this region that enhances either the fitness of the satRNA or its ability to effect TCV movement remains a possibility.

Testing possible interaction between H4a and H4b. The results of the H4a SELEX suggested that a hairpin is preferred in this location for satC replication in protoplasts, while emergence of sequence J indicated that the region is also involved in an additional effect that led to selection of this particular sequence/structure. As described above, sequence J contained some sequence identity with wt satC in the H4a stem, suggesting possible involvement of specific residues in an alternative conformation. We previously determined that replacing both H4a and H4b with the analogous hairpins from CCFV enhanced accumulation compared with replacing individual hairpins (39). Analysis of wt H4a and H4b sequence in satC revealed a possible alternative pairing involving sequence from both hairpins (positions 224 to 228 and 261 to 265) that is also present in CCFV H4a and H4b (Fig. 4A and data not shown). Interestingly, sequence J also maintains similar possible alternative pairing between the two hairpins (Fig. 4A).

To test if this alternative pairing is important for satC amplification in protoplasts, mutations were designed that disrupted potential base-pairing in one structure while maintaining the other structure (Fig. 4B). C226U, which was predicted to not significantly affect the H4a+H4b structure or the alternative structure, had no effect on satC replication (Fig. 4C). C243U, which was predicted to have little impact on the stem

of H4b in the H4a+H4b structure and no obvious effect on the stem of the alternative structure, reduced satC accumulation by 33% (Fig. 4C). G263A should impact both the stem of H4b in the H4a+H4b structure (Fig. 4B, left), as well as potentially disrupt the stem of the alternate structure (Fig. 4B, right). Of the three point mutations, G263A had the greatest impact on satC accumulation in protoplasts, reducing accumulation to 29% of wt (Fig. 4C). Combining C226U with G263A, which should be compensatory for the alternative structure, did not significantly improve the replication of satC (Fig. 4C). However, combining C243U with G263A, which was compensatory for the H4a+H4b structure, restored satC accumulation to 69% of wt. These results support the importance of maintaining the H4b stem for satC accumulation in protoplasts and do not provide evidence for the alternative structure. However, combining C226U, which by itself had no effect on satC accumulation, with C243U/G263A dramatically reduced accumulation to 3% of wt. This result was unexpected and suggested that H4a and H4b is more complex in terms of sequence, structure, and function than previously thought.

Two distinctive functional structures result from in vivo genetic selection of satC H4a+H4b. To further explore the relationship between satC H4a and H4b, satC with 45 randomized nucleotides representing the entire H4a and H4b region (positions 222 to 266) was transcribed and RNA was inoculated onto 30 turnip seedlings along with TCV genomic RNA. After 3 weeks, RNA was extracted from new leaves of 30 turnip plants. Nine distinct sequences, some with variants, were obtained from 29 clones recovered from round 1 plants (Fig. 5A), with sequences A_{ab} and B_{ab} being most abundant (but not found in later rounds). Sequence lengths ranged from 45 bases to 29 bases (i.e., a 16-nt deletion had occurred in sequence U_{ab}).

To allow for possible further evolution and competition with sequences not cloned in the initial population, four additional SELEX rounds were completed as described earlier for the H4a SELEX. Unlike the H4a SELEX, no clear winner emerged after five rounds. Clones isolated from rounds 3 and 5 represented three distinct sequences: related sequences $J_{ab} \rightarrow R_{ab}$, related sequences $V_{ab} \rightarrow Y_{ab}$, and related sequences Z_{ab}/AA_{ab} (Fig. 5A). Of these sequence winners, only related sequences Z_{ab}/AA_{ab} could potentially fold into H4a-like and H4b-like stem-loops, requiring the DR to form the H4a-like stem (Fig. 5B). In contrast, sequences $J_{ab} \rightarrow Q_{ab}$ and $V_{ab} \rightarrow Y_{ab}$ were predicted to fold into single hairpins that also incorporated the DR into the 5′ stem base. Mfold (41) prediction of full-length satC with either sequence X_{ab} (exemplifying the hairpin) or Z_{ab} (exemplifying the two stem-loops) in place of H4a+H4b suggests that these SELEXed sequences can fold into the structures modeled in Fig. 5B (data not shown).

To determine the ability of selected sequences to accumulate in protoplasts, representatives of the three groups of round 3 winners (sequences K_{ab}, Q_{ab}, X_{ab}, and Z_{ab}) were transcribed and RNAs inoculated into protoplasts with TCV genomic RNA. While no round 3 winner was able to accumulate to wt satC levels, accumulation of all selected sequences was significantly enhanced compared with satC containing either of two random H4a+H4b sequences ($Rd_{ab}1$ and $Rd_{ab}2$) (Fig. 5D).

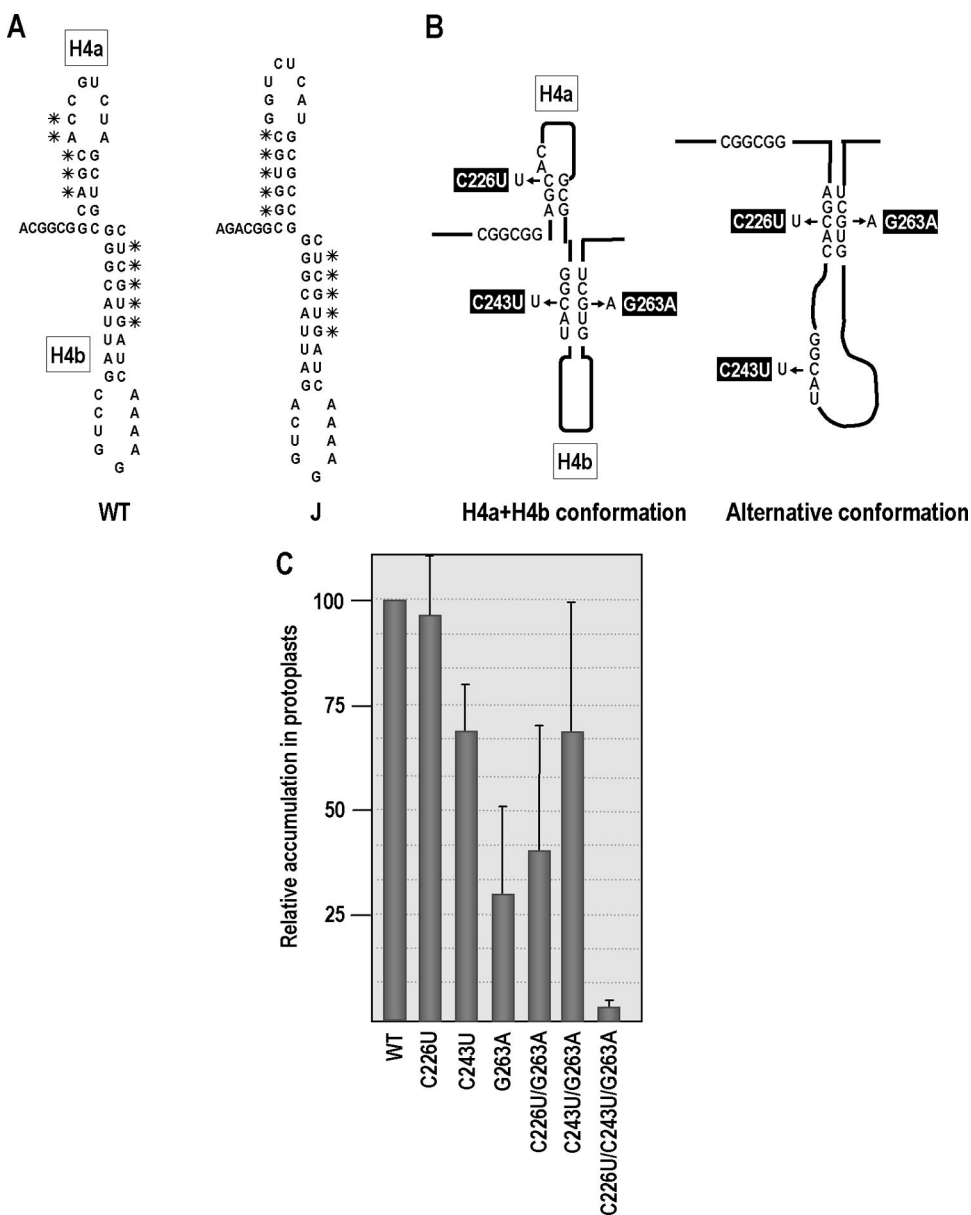In wt satC, the H4b loop forms an important pseudoknot

FIG. 4. Two potential conformations of satC H4a and H4b. (A) H4a and H4b regions of satC. Left, wt sequence; right, H4a SELEX winner sequence J. Asterisks denote possible alternate base-pairing interactions, as depicted for wt satC in panel B. (B) Two possible conformations for satC H4a+H4b. Boxes indicate satC mutations generated for analysis of accumulation in protoplasts. (C) Accumulation of satRNA (with various mutations) in protoplasts at 40 h postinfection. Mutations are indicated in panel B. Data from at least three independent experiments were normalized to wt satC levels. Standard deviations are indicated.

(ψ_2) with sequence adjacent to the 3′ side of the H5 stem (5′UCCG) (Fig. 1B) (39). When winning sequences were examined for nucleotides that could maintain this pseudoknot, both $J_{ab} \rightarrow Q_{ab}$ and Z_{ab}/AA_{ab} contained sequence that could maintain this pairing or extend it (3′-AGGC and 3′-GGGCU, respectively) (Fig. 5B). While $V_{ab} \rightarrow Y_{ab}$, which was structurally similar to $J_{ab} \rightarrow Q_{ab}$, did not have sequence that could form ψ_2, it did contain the similarly situated sequence 3′-CGGC (Fig. 5B). Examination of the sequence at the base of H5 in the $V_{ab} \rightarrow Y_{ab}$ winners revealed that seven of eight contained a second-site mutation at satC position 312 that converted the ψ_2 sequence 5′-UCCG to 5′-GCCG, which was capable of re-

forming the pseudoknot. These results support selection for maintenance of ψ_2 in the H4a+H4b SELEX winners.

The poorest-replicating sequence was Q_{ab} (9% of wt satC levels), which differed in sequence from K_{ab} (42% of wt satC levels) by only 3 nt. To determine which nucleotides were responsible for the enhanced accumulation of sequence K_{ab}, point mutations found in K_{ab} were introduced into sequence Q_{ab} (Fig. 5C). The C-to-U change of the end of the 45-nt region (Q_{ab}-C45U) improved accumulation in protoplasts by threefold (Fig. 5D), while G33A enhanced replication to K_{ab} levels. Interestingly, G35A or a combination of G35A and G33A was more beneficial for Q_{ab} replication than when these
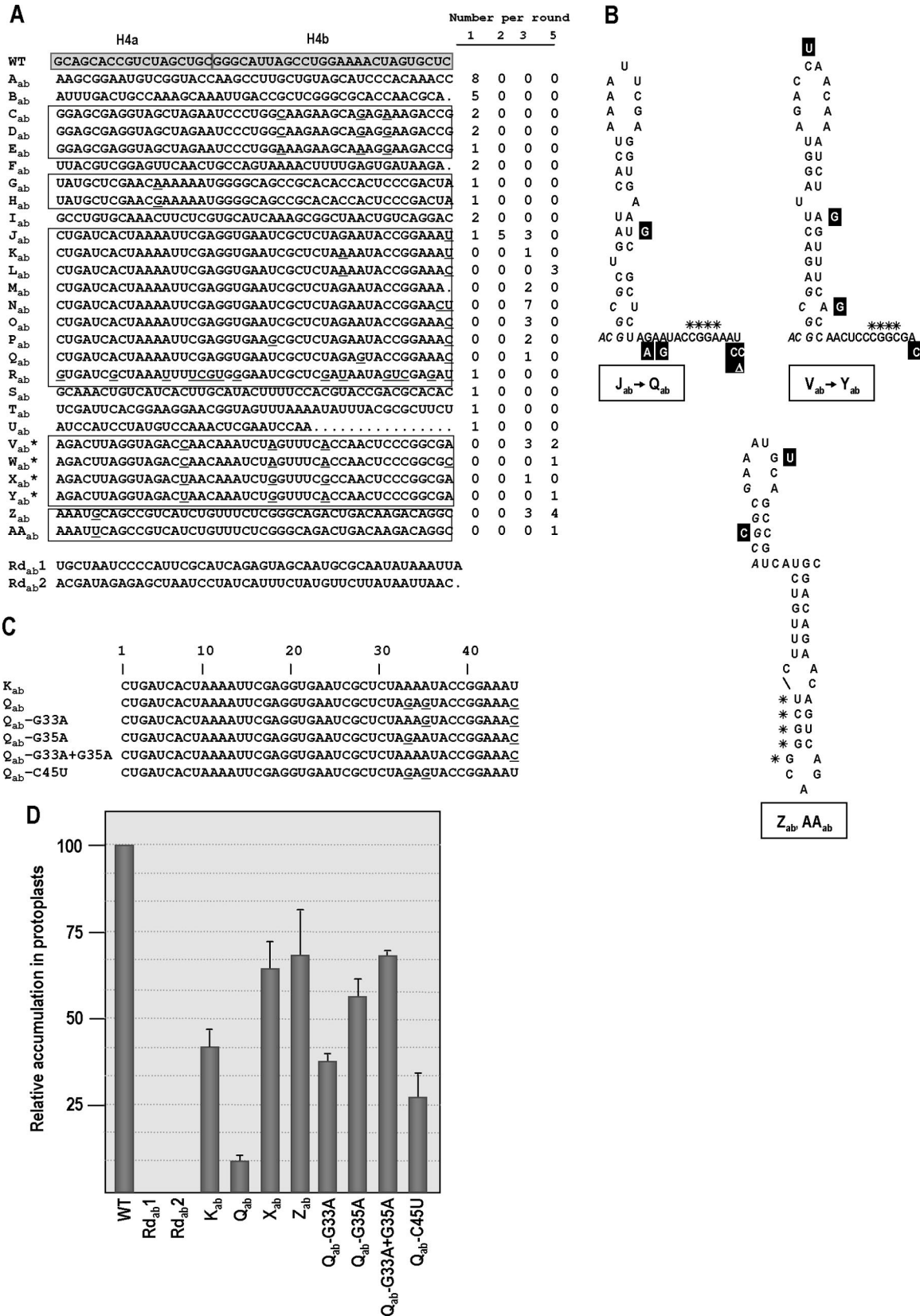
FIG. 5. In vivo genetic selection with randomized 45 nt of satC H4a+H4b results in recovery of different structural elements. (A) satC sequences obtained after SELEX rounds 1, 2, 3, and 5. The wt satC sequence is boxed and shaded at the top; the thin vertical line denotes the boundary between H4a and H4b. A$_{ab}$ through AA$_{ab}$ represent the 27 distinct cloned sequences, with related sequences boxed; underlined

base changes were combined with C45U. Since none of these changes is within the single hairpin or the putative ψ_2 region based on the model depicted in Fig. 5B, this result suggests that these downstream residues are interacting elsewhere in the satRNA, possibly as part of a preactive structure, promoting replication fitness.

Since K_{ab}, X_{ab}, and Z_{ab} did not replicate to wt satC levels in protoplasts, the three satC species were allowed to further evolve in planta. Transcripts from satC clones with sequences K_{ab}, X_{ab}, and Z_{ab} were independently transcribed and separately inoculated onto three turnip seedlings along with TCV genomic RNA. After three weeks, total RNA was extracted and a portion used to infect new plants. This protocol was repeated for a total of six rounds, with RNA from rounds 1 and 6 used to clone satC. After one round, the original K_{ab}, X_{ab}, and Z_{ab} sequences were preferentially cloned along with additional variants for K_{ab} and X_{ab} (Fig. 6A). After six rounds, no original K_{ab}, X_{ab}, and Z_{ab} sequences were detected, but rather newly evolved variants $K_{ab}B/K_{ab}C$, $X_{ab}B \rightarrow X_{ab}G$, and $Z_{ab}A \rightarrow Z_{ab}D$ were recovered. For $Z_{ab}A \rightarrow Z_{ab}D$, only one change (A37C) was found in the 45-nt region originally subjected to randomization (Fig. 6B, right). However, second-site mutations accumulated just 5′ of the DR in all but one variant, suggesting that this upstream A-rich sequence supports the function of the H4a+H4b region (Fig. 6A and B). Compared to parental K_{ab}, new variants $K_{ab}B/K_{ab}C$ had A33C and A44C changes and $K_{ab}C$ featured a U31C alteration that could have been retained from $K_{ab}A$ after round 1. These changes are all found 3′ of the hairpin (Fig. 6B, left). New variants $X_{ab}B \rightarrow X_{ab}G$ differed from parental X_{ab} by containing G44A. In addition, $X_{ab}B \rightarrow X_{ab}F$ had positions 13 to 16 (5′-ACUA) converted to CCC; these alterations occurred in the loop of the putative single hairpin (Fig. 6B, center). $X_{ab}G$ was distinctive in that it featured a 6-nt deletion, reducing the size of the modeled loop.

To determine if further evolution in planta enhanced replication of these satC, two or three evolved sequences from parentals K_{ab}, X_{ab}, and Z_{ab} were assessed for accumulation in protoplasts (Fig. 6C). While accumulation of Z_{ab} variants was not enhanced, a variant derived from K_{ab} ($K_{ab}B$) featured enhanced accumulation, and X_{ab} variants $X_{ab}B$ and $X_{ab}G$ accumulated to near-wt levels. This suggested that the changes in the terminal loop, poly(A) upstream region, and/or G44A of X_{ab} enhanced replication leading to selection in plants.

To determine which of the parental and round 6 evolved sequences were most fit in planta, direct competition experiments were performed. Equal amounts of transcripts from parentals $K_{ab}/X_{ab}/Z_{ab}$ or evolved variants $K_{ab}B/X_{ab}B/Z_{ab}B$ or $K_{ab}B/X_{ab}G/Z_{ab}B$ (comparisons between the latter two groups

allows for determination of the effect on fitness of the 6-nt deletion in the loop of $X_{ab}G$) were combined with TCV genomic RNA and inoculated onto three turnip seedlings. After 21 days, total RNA was extracted, and satC cDNA was cloned and sequenced. In the parental $K_{ab}/X_{ab}/Z_{ab}$ competition, 50 of 58 recovered clones were either X_{ab}, Z_{ab}, or newly derived variants (Fig. 7A), suggesting that higher accumulation of these sequences in protoplasts translates into enhanced fitness in plants (Fig. 5D and 6C). For the $K_{ab}B/X_{ab}B/Z_{ab}B$ and $K_{ab}B/X_{ab}G/Z_{ab}B$ competitions, $K_{ab}B$ was never recovered, indicating that the few changes in X_{ab} and Z_{ab} resulting in generation of $X_{ab}B$, $X_{ab}G$, and $Z_{ab}B$ allowed these variants to become much more functional than $K_{ab}B$ in plants. $X_{ab}G$ was not as competitive as $X_{ab}B$ when matched with $Z_{ab}B$, suggesting that the 6-nt deletion in $X_{ab}G$ (Fig. 7B) was not favorable for function. Overall, these results suggest that X_{ab}- and Z_{ab}-derived sequences (with the possible exception of $X_{ab}G$) are similarly competitive in planta (Fig. 7). This is intriguing, since structurally the two sequences appear dissimilar, with X_{ab} distinct compared to similarly structured wt H4a+H4b and Z_{ab}. Furthermore, the similar competitiveness of X_{ab} and Z_{ab} (and between sequences evolved from them) suggest that extending the H4a+H4b SELEX past five rounds might not have ultimately resulted in selection of a single winner.

Since $X_{ab}B$ accumulation approached levels of wt satC (Fig. 6C), the question arose whether $X_{ab}B$, with its distinct H4a+H4b structure compared to wt satC, could compete with wt satC in terms of movement in plants. To compare fitness, direct competition of wt satC and $X_{ab}B$ was performed. In addition, wt satC was also subjected to competition with K_{ab}, X_{ab}, Z_{ab}, $K_{ab}B$, and $Z_{ab}B$. In all six cases, wt satC was more fit than the SELEX winners at 21 dpi, as only wt satC was cloned (eight to nine clones each) from RNA isolated from leaves obtained from each in planta competition (data not shown). Therefore, although these six SELEX-derived satC RNAs accumulated in protoplasts to levels 42 to 100% of wt satC (Fig. 6C), specific elements within wt satC H4a and H4b must be critical for optimal fitness in plants.

DISCUSSION

The methodology of in vitro SELEX (systematic evolution of ligands by exponential enrichment) was initially developed to isolate individual RNAs from a large RNA pool that could bind to a specific target (5, 31). The principles of in vitro SELEX can be applied to in vivo evolution of viral RNAs, by randomizing a portion of viral sequence, introducing a pool of these randomized viral RNAs into host cells, and subsequently isolating functional RNAs. Melchers et al. (14) recently used in

nucleotides in the H4a+H4b region of these boxed sequences denote differences between the related clones. Periods denote absence of a base in a recovered sequence. Asterisks (V_{ab} through Y_{ab}) indicate the seven of eight clones that feature a second-site mutation at nt 312, just 3′ of H5, allowing for possible formation of ψ_2. The sequences of two random (Rd) H4a+H4b sequences cloned prior to selection in plants are noted. (B) Modeled structures of various cloned sequences. The 6 nt in italics at the 5′ end of all structures are part of wt satC that was not randomized in the SELEX procedure. Bases shown in black boxes are differences between sequences in the families shown. Asterisks denote nucleotides that can mediate formation of ψ_2. (C) Sequences of K_{ab}-, Q_{ab}-, and Q_{ab}-based derivatives. Numbers 33, 35, and 45 indicate positions within the 45-nt randomized region. Underlined nucleotides are differences in sequence Q_{ab} compared to K_{ab}. (D) Accumulation in protoplasts 40 h postinfection of wt satC, H4a+H4b SELEX winners K_{ab}-, Q_{ab}-, X_{ab}-, Z_{ab}-, and Q_{ab}-based derivatives, and satC with random (Rd$_{ab}$1 and Rd$_{ab}$2) H4a+H4b sequences. Data are from at least three independent experiments and were normalized to wt satC levels. Standard deviations are indicated.
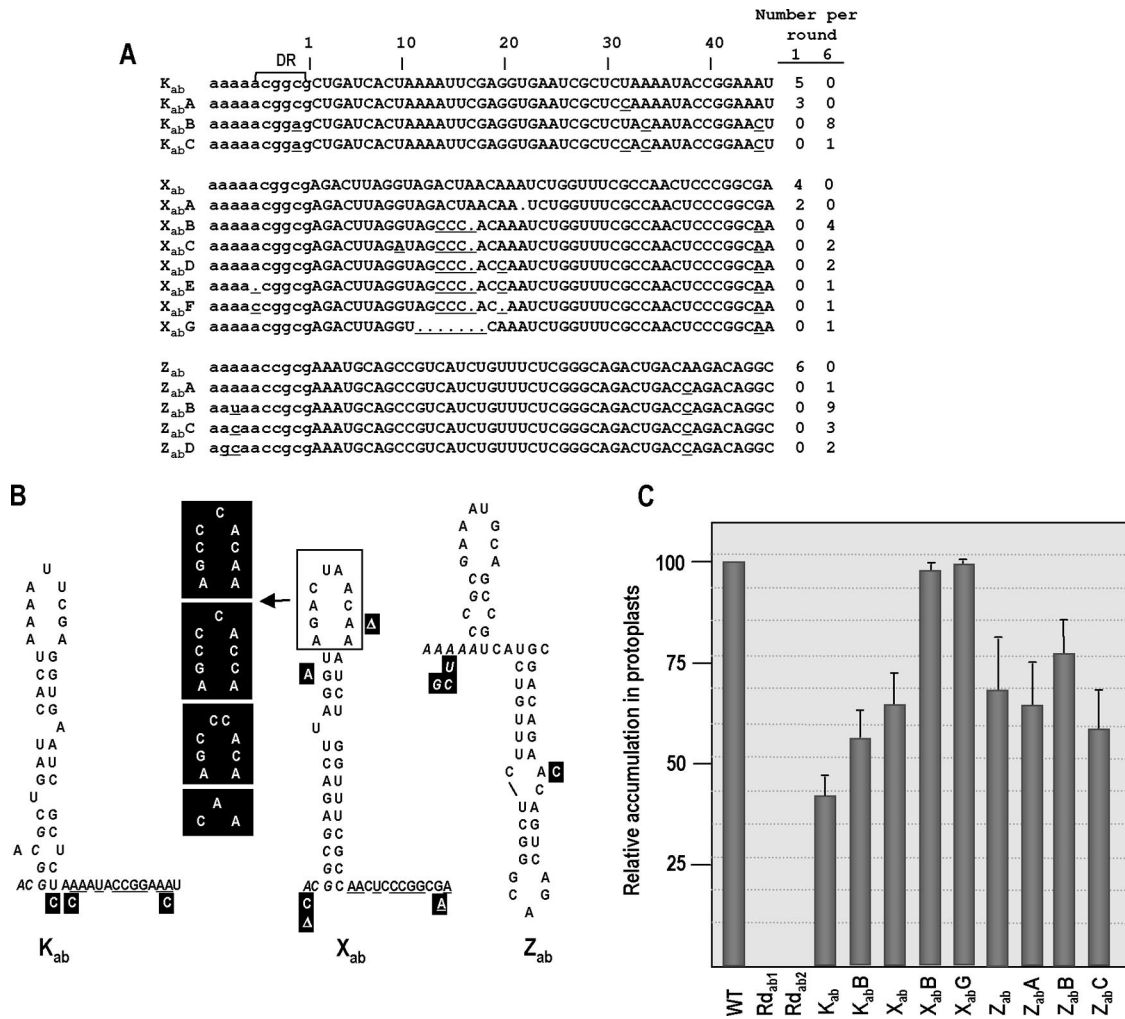
FIG. 6. Self-evolution of H4a+H4b SELEX third-round winners K_{ab} and X_{ab} markedly improves their accumulation in protoplasts. (A) Sequences cloned after the first and sixth rounds of 21-day infections in turnip. Lowercase letters indicate non-SELEXed sequence 5′ of H4a+H4b; underlined nucleotides and periods indicate changes or deletions, respectively, in nucleotides during evolution in planta. (B) Structural models of K_{ab}, X_{ab}, and Z_{ab}. Single nucleotide changes noted in panel A are indicated by black boxes adjacent to the site of the changed nucleotide. For X_{ab}, the loop is boxed and changes affecting this 10-nt region are depicted in black boxes. Underlined nucleotides in K_{ab} and X_{ab} indicate identical nucleotides at identical positions based on these models. (C) Accumulation in protoplasts 40 h postinfection of wt satC, H4a+H4b SELEX winners K_{ab}, X_{ab}, and Z_{ab}, selected sequences evolved from them, and satC with random H4a+H4b sequence ($Rd_{ab}1$ and $Rd_{ab}2$). Data are from at least three independent experiments and were normalized to wt satC levels. Standard deviations are indicated.

vivo SELEX to isolate a novel sequence for the evolutionarily conserved tetraloop D that interacts with poliovirus 3C protease and regulates viral RNA replication. Additionally, in vivo SELEX has been used extensively to characterize *cis*-acting sequences and structures in satC (1, 6, 7, 27, 29, 34, 37–39). Here, in vivo SELEX has allowed for in-depth characterization of the H4a and H4b region of satC.

Initial examination of satC H4a indicated that it is important for accumulation of the satRNA in protoplasts (39). Deletion of H4a reduced satC accumulation to 6% of wt, whereas replacing wt H4a with the reverse complement, which alters the loop sequence and maintains the wt stem, reduced accumulation to about 40% of wt levels. Replacing wt H4a with H4a from CCFV, which alters most of the stem and the lower bases in the loop, also reduced accumulation of satC to about 40% of wt levels in protoplasts (39). These data indicated that H4a is

an important *cis* element for robust satC RNA accumulation in plants and alterations in the stem and loop region can have a moderate effect on accumulation. It is also possible that changes in satC RNA sequence could alter RNA stability, and thus alter accumulation of satC. However, all previous examinations of mutant satC stability, including satC with large deletions, found no discernible differences from wt (33). In this experiment, H4a SELEX winner J, as well as related intermediate-round sequences G and E, contain selected sequence that can model into a single hairpin, and all sequences support satC accumulation to near wt levels in protoplasts (Fig. 2). The presence of sequences G and J in the later rounds and the emergence of sequence J as the SELEX winner suggests that a U:G pairing in the middle of the stem, found in J and G, is preferred over the A:U pairing found in sequence E. One of the two base differences between sequences J and G,
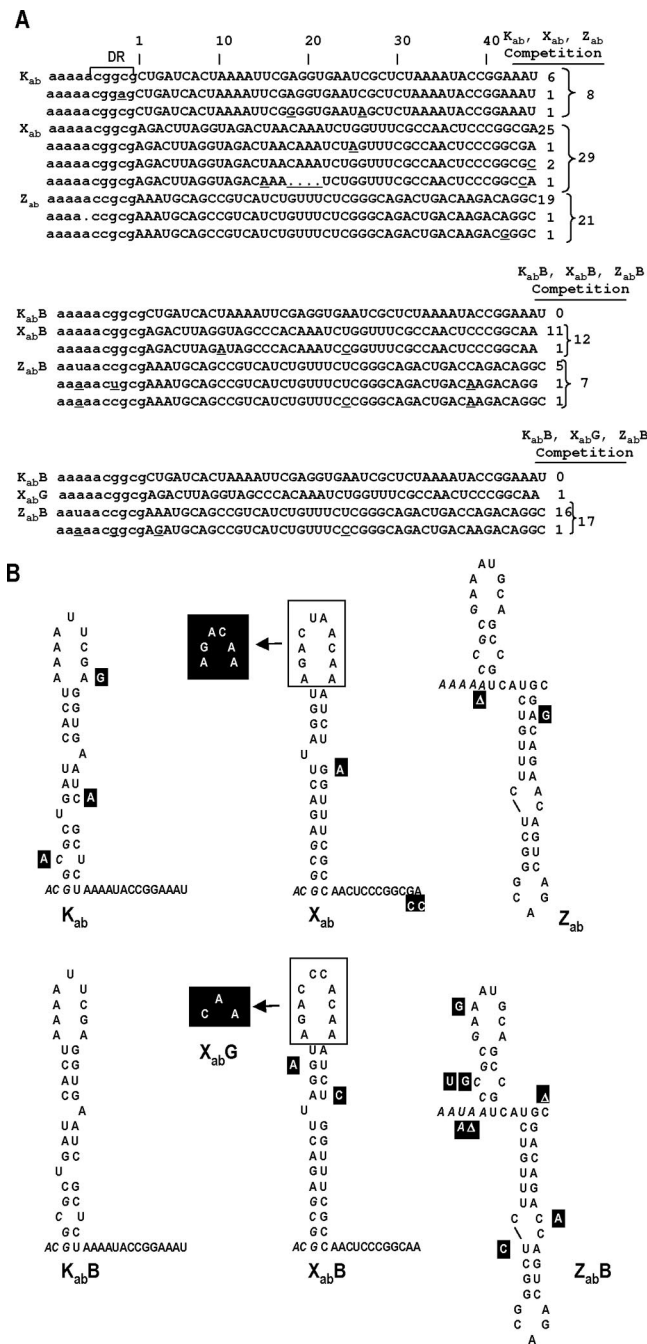
FIG. 7. Competitions of K_{ab}, X_{ab}, and Z_{ab} and evolved family members. All competitions began with inoculation of equal amounts of RNAs in a single-round, 21-day infection of three turnip seedlings before extraction of RNA. (A) Top, competition between K_{ab}, X_{ab}, and Z_{ab}. Middle, competition between $K_{ab}B$, $X_{ab}B$, and $Z_{ab}B$. Bottom, competition between $K_{ab}B$, $X_{ab}G$, and $Z_{ab}B$. (B) Structural models of K_{ab}, X_{ab}, Z_{ab}, $K_{ab}B$, $X_{ab}B/G$, and $Z_{ab}B$. Use of black boxes to denote single nucleotide changes (and loop for $X_{ab}B$ versus $X_{ab}G$) is as described for Fig. 6B.

located in the loop of the hairpin, enhances loop sequence similarity with wt H4a (5'-GUCU). This new base alteration in sequence J, along with the additional alteration upstream of the H4a region, did not enhance accumulation levels in

protoplasts (Fig. 2C), suggesting that these changes benefit the satRNA or the interaction of the satRNA with TCV in a different process.

Since these two differences in sequence J would permit formation of a TCV-like pseudoknot (Fig. 2B), we examined the analogous putative pseudoknot in wt satC for a role in accumulation in protoplasts (Fig. 3A). Genetic analyses did not support a TCV-like pseudoknot in this region of wt satC, and thus additional studies are required to determine if a putative pseudoknot exists in wt satC and sequence J that mediates a separate but important satRNA function. This pseudoknot in TCV (ψ_3) is critical for TCV accumulation in protoplasts, and disruption of the pseudoknot affects the 3' translational enhancer and ribosome binding to this element (26).

Interestingly, these experiments revealed that alteration of the H4a loop could complement mutations in the upstream DR element (Fig. 3). Prior results implicated the DR element as critical for satC transcription in vitro (35) by apparently contributing to the switch between satC preactive and active forms (39). We have recently determined that mutations in the DR-equivalent sequence in TCV disrupt single-site RdRp binding to the region (X. Yuan, M. Young, and A. E. Simon, unpublished data). One possibility is that the DR sequence is also important for RdRp binding to satC. Such an interaction could be restored in mutant C229G, where the CCG in the H4a loop is converted to CGG, which is repeated twice in the DR (CGGCGG). Interestingly, several of the hairpins selected in the H4a SELEX incorporated either a portion or the complete DR as part of the stem of the hairpin (Fig. 2B). Since there is no evidence for formation of H4a in the preactive structure of satC (35), it is possible that the DR sequence is accessible in the alternative configuration and available for RdRp binding.

Because the compensatory mutagenesis studies of H4a and H4b (Fig. 4) did not definitely resolve the conformation of this region of satC, the entire 45-nt region was subjected to SELEX and two types of winning sequences were obtained. The related sequences Z_{ab}/AA_{ab} are predicted to fold into H4a+H4b-like stem-loops, while $J_{ab}{\rightarrow}Q_{ab}$ and $V_{ab}{\rightarrow}Y_{ab}$ selected sequences model into single hairpins (Fig. 5). Examination of H4a+H4b-like Z_{ab} revealed a second-site mutation in the DR (G218C) that appeared in round 3 and was retained through round 5 and the six rounds of self-evolution (Fig. 6A). G218C was also seen in AA_{ab} (round 5). Interestingly, G218C reduces accumulation of wt satC by 72% and severely abrogates its in vitro transcription by the TCV RdRp (35). However, when a chimeric satC with H5 replaced by CCFV H5 was passaged in plants to improve fitness via acquisition of a second-site mutation(s), a more fit satC was recovered possessing G218C (39). One possibility is that acquisition of G218C allows for alternate control of the switch between preactive and active structures, which contributes to fitness of Z_{ab}.

Since the H4a+H4b region in genomic TCV RNA contributes to the TSS and binds ribosomes (13, 26), plasticity would not be expected for this region in TCV. The compact genomic organization of viruses often is recalcitrant to change, even though the RdRp mutation rate is high (2 × 10^{-5} to 1 × 10^{-4} per nt per replication event [4]). For

Tobacco etch virus, a survey of over 60 random single point mutations in the genome revealed that over 40% were lethal, and nearly half of the nonlethal mutations significantly impacted fitness in plants (2). Similar results were found in an in vitro study of vesicular stomatitis virus (19). Therefore, the plasticity of the satC H4a and H4b elements, represented by SELEX winners K_{ab} and X_{ab} and sequences evolved from them (especially $X_{ab}B$ due to its wt-level accumulation in protoplasts), is striking because of the size of the region randomized (45 nt), which represents 13% of its genome. Notably, the structural plasticity may have been possible because satC does not form the TSS and is not translated (26); therefore satC H4a+H4b sequences obtained in the SELEX only need to function in terms of replication and spread (and not translation). Reforming H4a+H4b into a single hairpin was associated with a similar 12-nt motif 3′ to the hairpin (5′-AAXUXCCGGXAA) (Fig. 6B). Within this motif is either 5′-CGGA (K_{ab}), which can mediate formation of ψ_2 with wt ψ_2 sequence at the 3′ base of H5, or 5′-CGGC, which can form a similar pseudoknot with ψ_2 sequence containing the second-site mutation near the 3′ base of H5 that was found in X_{ab}. The partial sequence similarity of the 12-nt motif in K_{ab} and X_{ab} may also suggest interaction of a portion of this motif with sequence elsewhere in the satRNA, permitting H4a+H4b to exist as a single hairpin as long as the ability to form a preactive structure that contains ψ_2 is retained. Further SELEX involving randomizing satC H4a+H4b along with other regions of satC might reveal whether additional interactions of the H4a+H4b region with upstream sequences are necessary to produce a functional, replicating RNA.

REFERENCES

1. **Carpenter, C. D., and A. E. Simon.** 1998. Analysis of sequences and predicted structures required for viral satellite RNA accumulation by *in vivo* genetic selection. Nucleic Acids Res. **26:**2426–2432.
2. **Carrasco, P., F. de la Iglesia, and S. F. Elena.** 2007. Distribution of fitness and virulence effects caused by single-nucleotide substitutions in *Tobacco etch virus*. J. Virol. **81:**12979–12984.
3. **Claus, C., W.-P. Tzeng, U. G. Liebert, and T. K. Frey.** 2007. Analysis of the selective advantage conferred by a C-E1 fusion protein synthesized by rubella virus DI RNAs. Virology **369:**19–34.
4. **Drake, J. W., and J. J. Holland.** 1999. Mutation rates among RNA viruses. Proc. Natl. Acad. Sci. USA **96:**13910–13913.
5. **Ellington, A. D., and J. W. Szostak.** 1990. In vitro selection of RNA molecules that bind specific ligands. Nature **346:**818–822.
6. **Guan, H., C. D. Carpenter, and A. E. Simon.** 2000. Analysis of *cis*-acting sequences involved in plus-strand synthesis of a *Turnip crinkle virus*-associated satellite RNA identifies a new *Carmovirus* replication element. Virology **268:**345–354.
7. **Guan, H., C. D. Carpenter, and A. E. Simon.** 2000. Requirement of a 5′-proximal linear sequence on minus strands for plus-strand synthesis of a satellite RNA associated with *Turnip crinkle virus*. Virology **268:**355–363.
8. **Hacker, D. L., I. T. D. Petty, N. Wei, and T. J. Morris.** 1992. Turnip crinkle

9. **Havelda, Z., C. Hornyik, A. Válóczi, and J. Burgyán.** 2005. Defective interfering RNA hinders the activity of a tombusvirus-encoded posttranscriptional gene silencing suppressor. J. Virol. **79:**450–457.
10. **Li, X. H., L. A. Heaton, T. J. Morris, and A. E. Simon.** 1989. Turnip crinkle virus defective interfering RNAs intensify viral symptoms and are generated *de novo*. Proc. Natl. Acad. Sci. USA **86:**9173–9177.
11. **Martínez-Salas, E., A. Pacheco, P. Serrano, and N. Fernandez.** 2008. New insights into internal ribosome entry site elements relevant for viral gene expression. J. Gen. Virol. **89:**611–626.
12. **McCormack, J. C., and A. E. Simon.** 2004. Biased hypermutagenesis associated with mutations in an untranslated hairpin of an RNA virus. J. Virol. **78:**7813–7817.
13. **McCormack, J. C., X. Yuan, Y. G. Yingling, W. Kasprzak, R. E. Zamora, B. A. Shapiro, and A. E. Simon.** 2008. Structural domains within the 3′ UTR of Turnip crinkle virus. J. Virol. **82:**8706–8720.
14. **Melchers, W. J. G., J. Zoll, M. Tessari, D. V. Bakhmutov, A. P. Gmyl, V. I. Agol, and H. A. Heus.** 2006. A CGUA tetranucleotide loop found in the poliovirus *ori*L by in vivo SELEX (un)expectedly forms a YNMG-like structure: extending the YNMG family with GYYA. RNA **12:**1671–1682.
15. **Miller, W. A., Z. Wang, and K. Treder.** 2007. The amazing diversity of cap-independent translation elements in the 3′-untranslated regions of plant viral RNAs. Biochem. Soc. Trans. **35:**1629–1633.
16. **Miller, W. A., and K. A. White.** 2006. Long-distance RNA-RNA interactions in plant virus gene expression and replication. Annu. Rev. Phytopathol. **44:**447–467.
17. **Oh, J. W., Q. Kong, C. Song, C. D. Carpenter, and A. E. Simon.** 1995. Open reading frames of turnip crinkle virus involved in satellite symptom expression and incompatibility with Arabidopsis thaliana ecotype Dijon. Mol. Plant-Microbe Interact. **8:**979–987.
18. **Qu, F., T. Ren, and T. J. Morris.** 2003. The coat protein of turnip crinkle virus suppresses posttranscriptional gene silencing at an early initiation step. J. Virol. **77:**511–522.
19. **Sanjuán, R., A. Moya, and S. F. Elena.** 2004. The distribution of fitness effects caused by single-nucleotide substitutions in an RNA virus. Proc. Natl. Acad. Sci. USA **101:**8396–8401.
20. **Shapiro, B. A., D. Bengali, W. Kasprzak, and J. C. Wu.** 2001. RNA folding pathway functional intermediates: their prediction and analysis. J. Mol. Biol. **312:**27–44.
21. **Shapiro, B. A., J. C. Wu, D. Bengali, and M. J. Potts.** 2001. The massively parallel genetic algorithm for RNA folding: MIMD implementation and population variation. Bioinformatics **17:**137–148.
22. **Simon, A. E., and S. H. Howell.** 1986. The virulent satellite RNA of turnip crinkle virus has a major domain homologous to the 3′ end of the helper virus genome. EMBO J. **5:**3423–3428.
23. **Simon, A. E., M. J. Roossinck, and Z. Havelda.** 2004. Plant virus satellite and defective interfering RNAs: new paradigms for a new century. Annu. Rev. Phytopathol. **42:**415–437.
24. **Song, C., and A. E. Simon.** 1994. RNA-dependent RNA polymerase from plants infected with turnip crinkle virus can transcribe (+)- and (-)-strands of virus-associated RNAs. Proc. Natl. Acad. Sci. USA **91:**8792–8796.
25. **Song, C., and A. E. Simon.** 1995. Requirement of a 3′-terminal stem-loop in in vitro transcription by an RNA-dependent RNA polymerase. J. Mol. Biol. **254:**6–14.
26. **Stupina, V. A., A. Meskauskas, J. C. McCormack, Y. G. Yingling, B. A. Shapiro, J. D. Dinman, and A. E. Simon.** 2008. The 3′ proximal translational enhancer of turnip crinkle virus binds to 60S ribosomal subunits. RNA **14:**2379–2393.
27. **Sun, X., and A. E. Simon.** 2003. Fitness of a Turnip crinkle virus satellite RNA correlates with a sequence-nonspecific hairpin and flanking sequences that enhance replication and repress the accumulation of virions. J. Virol. **77:**7880–7889.
28. **Sun, X., and A. E. Simon.** 2006. A cis-replication element functions in both orientations to enhance replication of *Turnip crinkle virus*. Virology **352:**39–51.
29. **Sun, X., G. Zhang, and A. E. Simon.** 2005. Short internal sequences involved in RNA replication and virion accumulation in a subviral RNA of *Turnip crinkle virus*. J. Virol. **79:**512–524.
30. **Thomas, C. L., V. Leh, C. Lederer, and A. J. Maule.** 2003. Turnip crinkle virus coat protein mediates suppression of RNA silencing in *Nicotiana benthamiana*. Virology **306:**33–41.
31. **Tuerk, C., and L. Gold.** 1990. Systematic evolution of ligands by exponential enrichment: RNA ligands to bacteriophage T4 DNA polymerase. Science **249:**505–510.
32. **Zhang, C.** 1995. Ph.D. thesis. University of Massachusetts, Amherst.
33. **Zhang, F., and A. E. Simon.** 2003. Enhanced viral pathogenesis associated with a virulent mutant virus or a virulent satellite RNA correlates with reduced virion accumulation and abundance of free coat protein. Virology **312:**8–13.
34. **Zhang, G., and A. E. Simon.** 2003. A multifunctional turnip crinkle virus

virus genes required for RNA replication and virus movement. Virology **186:**1–8.

replication enhancer revealed by *in vivo* functional SELEX. J. Mol. Biol. **326:**35–48.

35. **Zhang, G., J. Zhang, A. T. George, T. Baumstark, and A. E. Simon.** 2006. Conformational changes involved in initiation of minus-strand synthesis of a virus-associated RNA. RNA **12:**147–162.

36. **Zhang, G., J. Zhang, and A. E. Simon.** 2004. Repression and derepression of minus-stand synthesis in a plus-strand RNA virus replicon. J. Virol. **78:**7619–7633.

37. **Zhang, J., and A. E. Simon.** 2005. Importance of sequence and structural elements within a viral replication repressor. Virology **333:**301–315.

38. **Zhang, J., R. M. Stuntz, and A. E. Simon.** 2004. Analysis of a viral replication repressor: sequence requirements for a large symmetrical loop. Virology **326:**90–102.

39. **Zhang, J., G. Zhang, R. Guo, B. A. Shapiro, and A. E. Simon.** 2006. A pseudoknot in a preactive form of a viral RNA is part of a structural switch activating minus-strand synthesis. J. Virol. **80:**9181–9191.

40. **Zhang, J., G. Zhang, J. C. McCormack, and A. E. Simon.** 2006. Evolution of virus-derived sequences for high-level replication of a subviral RNA. Virology **351:**476–488.

41. **Zuker, M.** 2003. Mfold web server for nucleic acid folding and hybridization prediction. Nucleic Acids Res. **31:**3406–3415.